Evaluation of the dynamic cone penetrometer to detect compaction in ripped soils

Citation for published version:
Beckett, C, Bewsher, S, Guzzomi, A, Lehane, B, Fourie, AB & Riethmuller, G 2018, 'Evaluation of the dynamic cone penetrometer to detect compaction in ripped soils' Soil and Tillage Research. DOI: 10.1016/j.still.2017.09.009

Digital Object Identifier (DOI):
10.1016/j.still.2017.09.009

Link:
Link to publication record in Edinburgh Research Explorer

Document Version:
Peer reviewed version

Published In:
Soil and Tillage Research

Evaluation of the dynamic cone penetrometer to detect compaction in ripped soils

C.T.S. Beckett[a,], S. Bewsher[b], A. L. Guzzomi[c], B.M. Lehane[a], A.B. Fourie[a], G. Riethmuller[d]

[a]*School of Civil, Environmental and Mining Engineering, University of Western Australia, Perth, WA*
[b]*Main Roads WA*
[c]*School of Mechanical and Chemical Engineering, University of Western Australia, Perth, WA*
[d]*Department of Agriculture and Food, Government of Western Australia, WA*

Abstract

Land degradation due to compaction is a critical issue facing 21[st] century agriculture. Deep ripping is a popular solution to remediate compacted Western Australian soils. However, these soils are particularly susceptible to recompaction under vehicle traffic: reliable methods to detect and monitor compaction are therefore needed to inform remediation strategies.

Cone penetrometer testing (CPT) is a popular method to detect compaction under vehicle traffic in a range of soil conditions. However, traditional CPT equipment is unsuitable for large-scale use due to its expense and bulk. Dynamic penetrometers circumvent this issue by being inexpensive and man-portable. Such devices have seen recent success in determining properties of soft geotechnical materials but little is known of their performance in ripped soils. This study evaluated the ability of the “PANDA 2” dynamic penetrometer to detect compaction in ripped soils after the passage of aMassey Ferguson four-tonne tractor, which was typical of vehicles used at the test site. Two test sites of contrasting soil types were identified which had previously been ripped and left fallow and untrafficked for several years. Penetration resistance was measured along a high-resolution grid prior to trafficking and after one and five vehicle passes and compared to results from trial pits. Laboratory testing also examined the device's accuracy at shallow depths under controlled conditions. Results showed that the PANDA 2 was able to detect significant changes in penetration resistance after trafficking. However, several limitations on the device's use when interpreting field data were identified. Based on the findings of this study, dynamic penetrometers are not recommended to monitor compaction in ripped soilsfor the weight of vehicle used here. However, the devices may be of use when examining the passage of heavier vehicles.

Keywords: Deep ripping, Soil compaction, Cone penetrometer, Vehicle traffic

1. Introduction

Land degradation is an issue that is gaining recognition globally as a threat to food security. Causes of degradation are numerous: chemical factors, such as changing soil mineralisation and non-wetting behaviour; biological changes, such as variation in the soil organic content; and physical changes, such as soil erosion and compaction (Håkansson et al., 1988; Gretton and Salma, 1996; Hamza and Anderson, 2005). Degradation due to soil compaction, brought about through intensive cropping, short cropping cycles and increased vehicle and herd sizes, is of particular concern for Western Australia (WA), threatening over three quarters (roughly *eight million* hectares) of WA's agricultural land (Hall et al., 2010; Davies and Lacey, 2011).

Email addresses: `christopher.beckett@uwa.edu.au` (C.T.S. Beckett), `sam.bewsher@gmail.com` (S. Bewsher), `andrew.guzzomi@uwa.edu.au` (A. L. Guzzomi), `barry.lehane@uwa.edu.au` (B.M. Lehane), `andy.fourie@uwa.edu.au` (A.B. Fourie), `glen.riethmuller@agric.wa.gov.au` (G. Riethmuller)

“Deep ripping” is a popular technique to remediate soil compaction by shattering dense subsoil horizons and hardpans. Unlike ploughing, it does not invert the soil profile, but loosens it to reduce density (increase void space) and permit free movement of air (Ellington, 1987). Ripping is well suited for duplex soils (that is, soils whose lower horizons show an abrupt increase in clay content) as it elevates underlying clayey soil and buries water-repellent topsoil layers (Ellington, 1986). Although an expensive procedure, ripping has been shown to result in increased crop yields for Australian soils on a number of occasions (Davies et al., 2010; Hall et al., 2010). A disadvantage is that ripped soils are particularly susceptible to recompaction, particularly if controlled traffic practices cannot be employed due to practical or economic restrictions (Blackwell et al., 2013). Soil compaction states should therefore be monitored to employ ripping most effectively.

Cone Penetrometer Testing (CPT) is a popular method to assess the severity of soil compaction under traffic in virgin (Grunwald et al., 2001; Raper, 2005; Patel and Mani, 2011), tilled (Ehlers et al., 1983; Aase et al., 2001) and ripped soils (Ellington, 1986; Lardner and Tibbett, 2013). Several designs of penetrometer exist, however all fundamentally measure the force required to drive the device vertically down through the soil profile. Traditional CPT requires the use of a heavy vehicle from which the cone is driven into the ground at a constant velocity (“static” CPT). Such devices are not readily usable for agricultural land, in part due to their weight and effect on compaction but also their cost (Herrick and Jones, 2002). Manual static penetrometers exist butskill is needed in their operation to control penetration speed. The “dynamic” penetrometer was developed to circumvent these issues. In Dynamic Cone Penetrometer Testing (DCPT), the device is driven into the ground by repeated hammering; the kinetic energy delivered to the device is used to determine soil resistance when combined with device parameters (e.g. cone diameter and angle etc.). The first dynamic penetrometers were designed to operate with an automated hammer, delivering constant kinetic energy per blow: the large accompanying rigs were unsuitable for agricultural work. Modern designs, however, are hand-held and can be used by a single operator manually delivering hammer blows. As such, they are suitably mobile (and inexpensive) to be deployed for use in soft soils, for example mine tailings (Villavicencio and Lemus, 2013), railway ballast (Cui, 2016) and temporary working platforms (Kazmee et al., 2016).

Penetrometer resistance, q_c (or q_d for DCPT), is affected by soil density and so can give a measure of soil compaction when compared to historic data; it cannot be converted to density directly as resistance is also strongly affected by soil composition and water content (Yu and Mitchell, 1998; Pournaghiazar et al., 2013; Robertson and Cabal, 2015). Although some precautions are taken to ensure similar water contents with depth (e.g. Henderson et al. (1988)), penetrometer results are likely to remain highly variable in tilled or ripped soil where fractured elements of differing density and water retention might persist (Dexter, 1997).

This paper examines the ability of a hand-held, single-operator "PANDA 2" dynamic penetrometer (Sol Solution, 2012) to detect compaction in ripped agricultural soils. Two sites of differing soil types were identified which had previously been ripped and left fallow for two years. DCPT results were obtained prior to traffic and following one and five passes of an agricultural vehicle and compared to density and water content measurements from trial pits. DCPT repeatability was also assessed via laboratory testing under controlled conditions. The experimental programme is described in the following section, after which results from the study's laboratory and field components are presented and implications for compaction detection using DCPT discussed.

2. Experimental procedure

2.1. Site selection

The "Eco Restoration" zone (ER) at The University of Western Australia (UWA) Farm Ridgefield was used for testing. The region has a Köppen-Geiger Climate Classification of Csa (temperate with distinctly dry and hot summers), which is typical of the Western Australian wheat belt (Peel et al., 2007), and experiences a mean annual average rainfall of 426 mm, predominantly in the winter months (Australian Government Bureau of Meteorology, 2015). The predominant soil types are loamy sands with sandy clays (United States Department of Agriculture classifications) present in a strip through the centre of the site. Two test areas, A and B, of contrasting soil types were identified: both were deep ripped to a depth of approximately **300 mm in 2010** and then left fallow and untrafficked. **Rip lines were spaced at approximate 2 m intervals (Perring et al., 2012).** Soil cores at Sites A and B, obtained during the ER project, indicated a soil depth in excess of 1.9m with similar soil textures throughout. Sites were orientated to allow traffic to follow a constant contour. The ER zone and the locations and orientations of Sites A and B are shown in Figure 1.

(Insert Figure 1 somewhere near here)

2.2. Field testing

A hand-held "PANDA 2" DCPT device (90° cone angle, projected cone area 200 mm^2, ∅16 mm head, **∅14 mm shaft**), capable of measuring cone resistances $q_d \leq 30$ MPa, was used to measure dynamic penetration resistance before and after the passage of an agricultural vehicle. The PANDA 2 can be used by a single operator, making it useful for large-scale field testing as shown in Figure 2. The operator hammers the penetrometer shaft into the substrate using a cushioned mallet. The PANDA 2's onboard computer converts the strike energy and load measured at the device's tip into penetration resistance. Undrained shear strengths calculated from PANDA 2 data have been shown to correlate well with traditional static CPT results (Langton, 1999). Penetrometer readings were obtained at each test site for three conditions: no traffic ("Test 1"); one pass of an agricultural vehicle ("Test 2"); and five passes of the same vehicle ("Test 3"). Traffic intensity was selected following results from Bakker and Davis (1995) (reported in Hamza and Anderson (2005)), who observed that the majority of compaction occurred after a single vehicle pass for tilled soils. The vehicle used to traffic the area was a Massey Ferguson MF6245 tractor, possessing 4WD capabilities with a loader shovel mounted to the front: vehicle details are given in Table 1.

(Insert Figure 2 somewhere near here)

(Insert Table 1 somewhere near here)

Identical grids were used to delineate testing locations at each site, shown in Figure 3. Each grid was divided into three groups. Each group comprised three 'runs', one for each tested condition, divided into eight sections delimiting each penetrometer test: a total of 72 penetrometer tests per site. The central run in each group was used for Test 1, straddled by those for Tests 2 and 3, separated by 500 mm. This arrangement reduced the likelihood of neighbouring penetrometer tests interfering with results whilst maintaining, as far as practicable, similar ground conditions per section per test. Penetration resistance was measured to a depth of 600 mm to ensure that the penetrometer passed through the full ripped profile.

(Insert Figure 3 somewhere near here)

Field testing occurred on the 4th and 5th of August 2014. Water content in the fields was high following 219 mm of rainfall over the preceding 3 months (determined from on-site measurement), which was consistent with the long term averages for the area (Australian Government Bureau of Meteorology, 2015). New vegetation growth on both sites was evident and was attributable to the recent rainfall for the region. All 144 tests were completed within 24 hours by a single operator: a testament to the PANDA 2's deployability.

Two trial pits were dug on each site to measure density and water content prior to traffic (Test 1) and after trafficking (Test 3, one pit per test). Sampling followed AS1289.1.3.1 (Standards Australia, 1999) using a greased, thin-walled sampling device of internal diameter 53 mm. Pits were dug to a depth of 700 mm at the end of the 6th test section to obtain samples from under the vehicle tramline (Figure 3). Soil was sampled at depths of 200, 400 and 600 mm below the surface. **Trial pits showed no indication of large soil clods above the ripping line: rather, the soil texture was largely uniform**.

2.3. Laboratory testing

Laboratory tests examined penetration measurement variability under controlled conditions. Such tests were necessary given the potentially heterogeneous nature of the ripped soils and the need to discern site variability from that of the device. Soil from Site A was compacted into a ∅300 mm by 550 mm column in 50 mm layers of known mass and volume to a dry density of 1813 kgm^{-3} at 12% water content (previously determined to be the optimum water content (Standard compaction test, AS1289.5.1.1) for this density). The column was then left to equilibrate at 21°C, 98% relative humidity for 14 days to establish constant suction throughout. After equilibration, four penetrometer tests were carried out using the PANDA 2, equally spaced about the column centre with a minimum of 100 mm between the device and the column wall. Columns were penetrated to nominal depths of 450 mm to prevent the base interfering with results or damaging the device (Bolton and Gui, 1993). Results were used to understand device accuracy in the field, discussed in the following sections. It is noted that such conditions are not representative of field conditions: higher densities than those in the field were selected to reduce the chance of densification during penetration; high humidity was used to produce low suctions and so reduce the risk of elevating penetration resistance above that that could be measured.

3. Results and Discussion

3.1. Device accuracy

Results from laboratory soil column testing are shown in Figure 4. No one test consistently produced higher or lower resistances, suggesting that test separation distances were sufficient. However, results were highly variable with depth. Raw data was therefore smoothed using a moving average over a 5 mm depth interval. Raw and smoothed penetrograms are compared in the left-hand plot in Figure 4. Mean penetration resistance and standard deviation were calculated for smoothed data; mean values are also shown to the left of Figure 4.

(Insert Figure 4 somewhere near here)

Overall, penetration resistance increased with depth, as expected. However, deviations about the mean also increased with depth, shown to the right of Figure 4 as a shaded region of ± 1 standard deviation about the mean. As material density and suction were controlled and constant with depth (as far as practicable), deviations were indicative of the device's performance: one of the major factors affecting q_d is the level of confinement, i.e. such behaviour may have been due to changes in confinement stresses at shallow depths (Bolton and Gui, 1993). A simple linear function was derived to describe changing uncertainty with depth:

$$\mathrm{SD}(z) = 0.0026z + 0.05 \text{ (MPa)} \tag{1}$$

where SD(z) is standard deviation as a function of depth, z, in mm. Eqn 1 applied to the linearised mean penetration resistance is shown superimposed on smoothed data to the right of Figure 4. It is likely that the form of Eqn 1 would change if higher penetration resistances or greater depths were encountered: the application of Eqn 1 to field data and its implications on data reliability are discussed in the following sections. Note that linear averaging produced a non-zero resistance at the surface, which is not possible in reality (Biarez and Gresillon, 1972): linear averaging is only used diagrammatically in Figure 4 to show the effect of Eqn 1 on uncertainty. Surface resistance was forced through zero during moving-average smoothing for subsequent analyses.

3.2. Field testing

Raw penetration profiles for Sites A and B are shown in Figures 5 and 6: for brevity, only results for sections 3 and 6, i.e. those results taken on the vehicle tramlines (Figure 3), are included. As for laboratory data, field penetration profiles displayed erratic changes in penetration resistance with depth. The "rlowess" smoothing method was therefore also applied to field data, again shown in Figures 5 and 6. Mean smoothed penetration resistances and their standard deviations for tests 1 to 3 are shown in Figure 7 (again, sections 3 and 6 only).

(Insert Figure 5 somewhere near here) (Insert Figure 6 somewhere near here) (Insert Figure 7 somewhere near here)

Results from trial pits at Sites A and B are given in Table 2. Pits at both sites detected increases in density after trafficking: roughly 9% at Site A and 4% at Site B. At Site A, the degree of saturation (S_r) was lower nearer the surface due to slight drainage but dry density (ρ_d) was similar throughout the profile. ρ_d and S_r increased by similar amounts after trafficking at all depths, which was consistent with compaction. Site B conditions were more variable than Site A: ρ_d apparently reduced marginally at 400 mm after trafficking. The slight reduction was indicative of the variability of the ripped layer: on average, density increased throughout the profile. ρ_d at 600 mm was particularly high, suggesting that some densified fragments may have survived from historic processes: a highly heterogeneous layer existing below 400 mm is suggested by large standard deviations in Figure 7 for Site B, section 6. This depth coincided well with the reported ripping depth of approximately 400 mm at each site. For both sites, degree of saturation was largely consistent with depth for all tests (excepting the cases already mentioned), indicating good conditions for penetrometer testing (Henderson et al., 1988). Densities prior to traffic suggest that root growth of agricultural species would not be impaired at either site (Daddow and Warrington, 1983; Davies and Lacey, 2011). However, densities after 5 passes may inhibit root growth, depending on the species and compaction conditions.

(Insert Table 2 somewhere near here)

3.3. Identifying compaction

Penetrometer resistances fell between similar ranges for laboratory and field testing (both sites): Eqn 1 could therefore reasonably describe device variability at Sites A and B. Deviations were combined as the square root of the sum of the variances per depth: mean penetration resistances per depth were unaltered.

The same process was applied to all averaged penetration profiles. Figure 8 shows an example effect of incorporating Eqn 1 on overall standard deviations (Site A, section 3 after zero vehicle passes).

(Insert Figure 8 somewhere near here)

A paired t-test was used to identify significant changes in q_d with depth on trafficking. Differences between zero and one and zero and five vehicle passes were analysed. p values below 0.05 were interpreted as significant evidence of compaction: anything above 0.05 could not reliably be said to be due solely to trafficking. p values determined between q_d after zero and five passes are shown in Figure 9 where contours at $p \leq 0.05$ (grey) and $p \leq 0.01$ (black) were drawn between the eight sections. No significant q_d differences were found between zero and one pass at any depth (i.e. $p > 0.05$ at all points): given that Bakker and Davis (1995) anticipated the majority of compaction to occur after one pass, this result was unexpected. Implications of not detecting compaction are discussed at the end of this paper.

(Insert Figure 9 somewhere near here)

At both sites, significant changes in q_d between tests 1 and 3 were clustered around the sections immediately underneath the tyres (numbers 3 and 6), as expected. From unmodified field data, some significant differences arose in Site A below 200 mm depth. However, significant results below depths of 200 mm were all but eliminated when including device variability (lower plots in Figure 9), demonstrating the need to consider the device's performance when interpreting q_d data. Notably, results for section 3 were far stronger than those for section 6 at both sites. Section 3 was underneath the vehicle's left-hand tyre during trafficking, at a lower elevation: the vehicle's tilt shifted more of its weight onto the downhill tyre. At Site A, significance was also strong for penetrometer tests along section 4, suggesting that the vehicle's tyres passed between the two. Correlation to trial pit results was, however, poor: no significant q_d changes were detected below 200 mm despite recorded changes in density. A possible cause was the commensurate change in S_r with ρ_d on compaction; increases in S_r indicate higher pore water pressures (either due to reduced suction or excess pressure following rapid compaction) which reduce q_d due to reduced effective stress (Bolton and Gui, 1993; Pournaghiazar et al., 2013). As no pore water pressure measurements were made this interpretation is only speculative, however it serves to highlight the limitations of depending on q_d to interpret density changes.

4. Concluding remarks

This paper presented a detailed study evaluating the PANDA 2 dynamic penetrometer's ability to detect compaction under agricultural traffic. Results demonstrated that the PANDA 2 was able to detect significant q_d changes in the upper 200 mm of the soil profile under the vehicle's wheels in differing soil types. However, q_d results did not reflect density changes detected in trial pits, attributed to the complex effects of density and soil water content on q_d, both of which change under compaction. The study also identified several limitations to the device's use in the field:

- A high resolution grid with well-controlled soil conditions was needed to extract meaningful q_d values. The luxury of such controls in reality is unlikely: q_d variability would therefore be greater than that found here.

- Multiple vehicle passes were required to detect significant q_d changes: multiple passes may induce excessive compaction before it can be identified. The

PANDA's sensitivity was not sufficient to detect relative density changes of 9% at Site A or 4% at Site B.

- Laboratory testing demonstrated that, for the range of depths investigated, device accuracy reduced with increasing depth. The penetrometer's error under controlled conditions must be accounted for when interpreting field q_d data. Error calibration must be completed prior to field testing and will likely vary with penetration resistance and probed depths.

- Changes in q_d could not reliably be detected in highly heterogeneous layers, for example pre-existing ripped material.

- Raw penetration profiles were erratic and required smoothing to interpret q_d values.

In light of these issues, it is unlikely that dynamic penetrometers can provide a 'one stop' solution detect compaction in ripped soils. However, field testing demonstrated that greater ground pressures, here due to vehicle tilt, improved results. Dynamic penetrometers may therefore be suited to detect compaction under **heavier** vehicle traffic **than that investigated here**, for example larger agricultural or mining vehicles.

5. Acknowledgements

The authors would like to thank Michael Perring and Tim Morald from the UWA School of Plant Biology for generously providing access to the UWA Farm Ridgefield and the Eco Restoration zone and for essential on-site support.

Aase, J. K., Bjornberg, D. L., Sojka, R. E., 2001. Zone-subsoiling relationships to bulk density and cone index on a furrow-irrigated soil. Trans. ASAE 44 (3), 577–583.

Australian Government Bureau of Meteorology, 2015. Monthly climate statistics, Pingelly, WA. [accessed: 06/01/2015].
URL http://www.bom.gov.au/climate/averages/tables/cw_010626.shtml

Bakker, D., Davis, R. J., 1995. Soil deformation observations in a Vertisol under field traffic. Aus. J. of Soil Res. 33, 817–832.

Biarez, J., Gresillon, J. M., 1972. Essais et suggestions pour le calcul de la force portante des pieux en milieu pulverulent. Géotechnique 22, 433–450.

Blackwell, P., Hagan, J., Riethmuller, G., Davies, S., Yokwe, S., 22–25 September 2013. Inegrating CTF into WA dryland cropping with dry autumns, increasing machinery scale and new tillage methods. In: Proceedings of the Society for Engineering in Agriculture Conference 2013. The Atrium Resort, Mandurah, Western Australia.

Bolton, M. D., Gui, M. W., 1993. The study of relative density and boundary effects for cone penetration tests in centrifuge. Tech. Rep. CUED/D-SOILS/TR256, University of Cambridge.

Cui, Y.-J., 2016. Unsaturated railway track-bed materials. ENPC, pp. 1–15.

Daddow, R., Warrington, G., 1983. Growth-limiting soil bulk densities as influenced by soil texture. Tech. rep., Watershed Systems Development Group, USDA Forest Service.

Davies, S., Lacey, A., 2011. Subsurface compaction: A guide for wa farmers and consultants. Tech. rep., Department of Agriculture and Food, Western Australia.

Davies, S., Newman, P., Best, B., 2010. Impact of soil inversion, soil dilution and claying on non-wetting sandplain soils. Tech. rep., Crop Updates (Department of Agriculture and Food, Western Australia and the Grains Research and Development Corporation).

Dexter, A. R., 1997. Physical properties of tilled soils. Soil Till. Res. 43 (1-2), 41–63.

Ehlers, W., Köpke, U., Hesse, F., Böhm, W., 1983. Penetration resistance and root growth of oats in tilled and untilled loess soil. Soil Till. Res. 3 (3), 261–275.

Ellington, A., 1986. Effects of deep ripping, direct drilling, gypsum and lime on soils, wheat growth and yield. Soil Till. Res. 8, 29–49.

Ellington, A., August 1987. Effects of deep ripping on cropping soils and crop production. In: Reeves, T. G. (Ed.), Responding to Change, Proceedings of the 4th Australian Agronomy Conference. Australian Society of Agronomy, La Trobe University, Melbourne, Victoria (Australia).

Gretton, P., Salma, U., 1996. Land degradation and the Australian agricultural industry. Tech.

rep., Commonwealth of Australia.

Grunwald, S., Rooney, D. J., McSweeney, K., Lowery, B., Mar. 2001. Development of pedotransfer functions for a profile cone penetrometer. Geoderma 100 (1–2), 25–47.

Håkansson, I., Voorhees, W. B., Riley, H., 1988. Vehicle and wheel factors influencing soil compaction and crop response in different traffic regimes. Soil Till. Res. 11 (3–4), 239–282.

Hall, D. J. M., Jones, H. R., Crabtree, W. L., Daniels, T. L., 2010. Claying and deep ripping can increase crop yields and profits on water repellent sands with marginal fertility in southern Western Australia. Aus. J. Soil Res. 48, 178–187.

Hamza, M. A., Anderson, W. K., 2005. Soil compaction in cropping systems: A review of the nature, causes and possible solutions. Soil Till. Res. 82 (2), 121–145.

Henderson, C. W. L., Levett, A., Lisle, D., 1988. The effects of soil water content and bulk density on the compactibility and soil penetration resistance of some western australian sandy soils. Aus. J. Soil Res. 26, 391–400.

Herrick, J. E., Jones, T. L., 2002. A dynamic cone penetrometer for measuring soil penetration resistance. Soil Sci. Soc. Am. J. 66 (4), 1320–1324.

Kazmee, H., Tutumluer, E., Haddani, Y., Navarrete, M., Gourves, R., 2016. Use of a variable energy penetrometer and geo-endoscopic imaging in the performance assessment of working platforms constructed with large size unconventional aggregates. In: Proceedings of the International Conference on Transport and Development. ASCE, pp. 1227–1238.
URL http://www.asce-ictd.org/

Langton, D. D., 1999. The PANDA: Light-weight penetrometer for soil investigation and monitoring material compaction. Tech. rep., Soil Solution Ltd.

Lardner, T. D., Tibbett, M., 2013. Deep ripping after topsoil return affects root proliferation and floristic diversity in a restored biodiverse forest after bauxite mining. In: Tibbett, M., Fourie, A. B., Digby, C. (Eds.), Mine Closure 2013. Australian Centre for Geomechanics, Perth, Cornwall, UK.

Patel, S., Mani, I., 2011. Effect of multiple passes of tractor with varying normal load on subsoil compaction. J. Terramech. 48 (4), 277–284.

Peel, M. C., Finlayson, B. L., McMahon, T. A., 2007. Updated world map of the Köppen-Geiger climate classification. Hydrol. Earth Syst. Sci. 11, 1633–1644.

Perring, M. P., Standish, R. J., Hulvey, K. B., Lori Lacha, T. K. M., Parsons, R., an Richard

J. Hobbs, R. K. D., 2012. The Ridgefield Multiple Ecosystem Services Experiment: Can restoration of former agricultural land achieve multiple outcomes? 163, 14–27.

Pournaghiazar, M., Russell, A., Khalili, N., 2013. The cone penetration test in unsaturated sands. Géotechnique 63 (14), 1209–1220.

Raper, R. L., 2005. Agricultural traffic impacts on soil. J. Terramech. 42 (3–4), 259–280.

Robertson, P. K., Cabal, K. L., 2015. Guide to cone penetration testing for geotechnical engineering. Gregg Drilling and Testing Inc.

Sol Solution, 2012.
URL `http://www.sol-solution.com/panda/58`

Standards Australia, 1999. AS1289.1.3.1-1999 : Methods of testing soils for engineering purposes - Sampling and preparation od soils - Undisturbed samples - Standard method.

Standards Australia, 2003. AS1289.5.1.1.-2003. Methods of testing soils for engineering purposes. Method 5.1.1: Soil compaction and density testsDetermination of the dry density/moisture content relation of a soil using standard compactive effort.

Villavicencio, R., Lemus, L., 2013. The PANDA technology applied to design and operation of tailings dams. In: Barrera, S., Niederhauser, M., Shaw, G., van Zyl, D., Wilson, W. (Eds.), Tailings2013. Gecamin, pp. 1–8.

Yu, H., Mitchell, J., 1998. Analysis of cone resistance: Review of methods. J. Geotech. Geoenviron. Eng. 124 (2), 140–149.

6. Figures

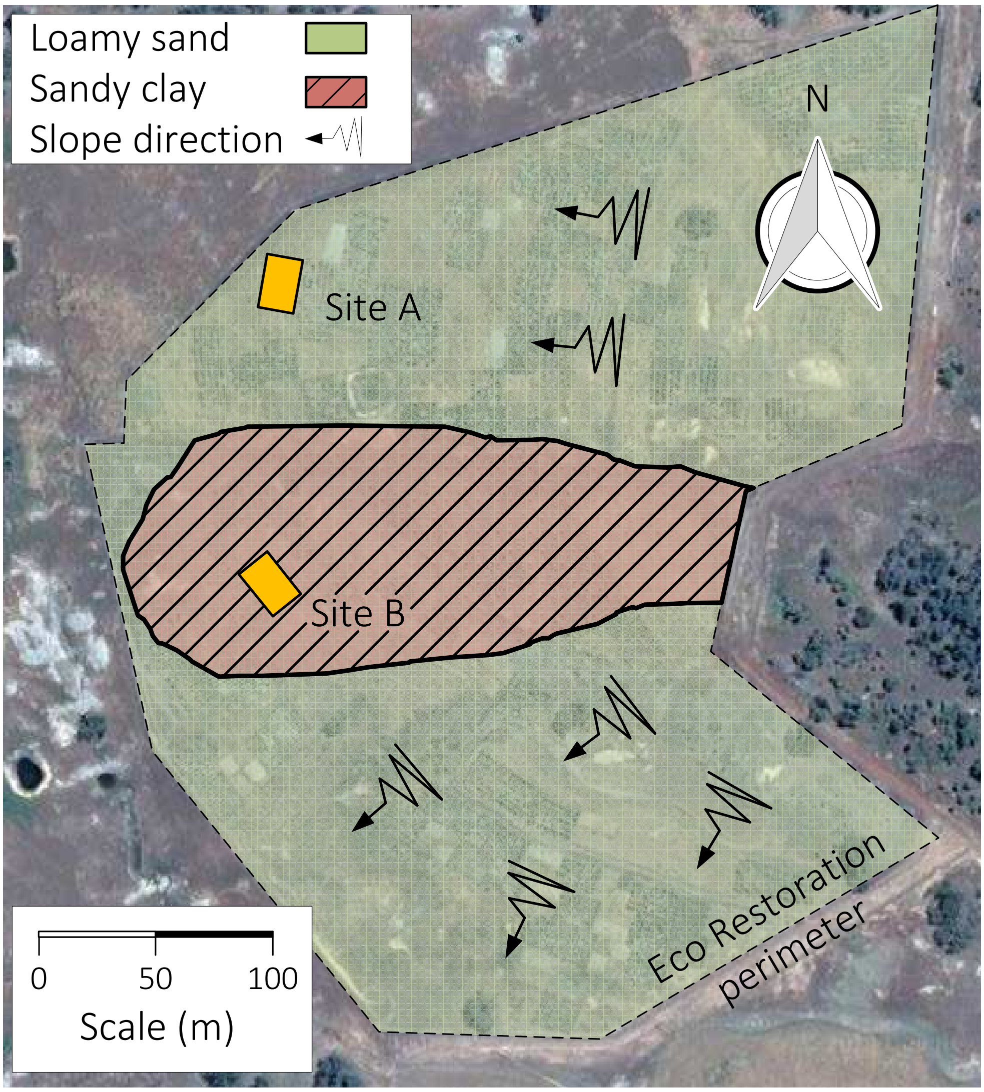

Figure 1: Aerial view of the UWA Farm Ridgefield Eco Restoration zone, showing soil types and test sites A and B

Figure 2: PANDA 2 operation on soft soil. The operator (left) has the mallet in his hand. The logger (bottom right) displays calculated resistance in real time. All equipment fits into the carrying case for transport.

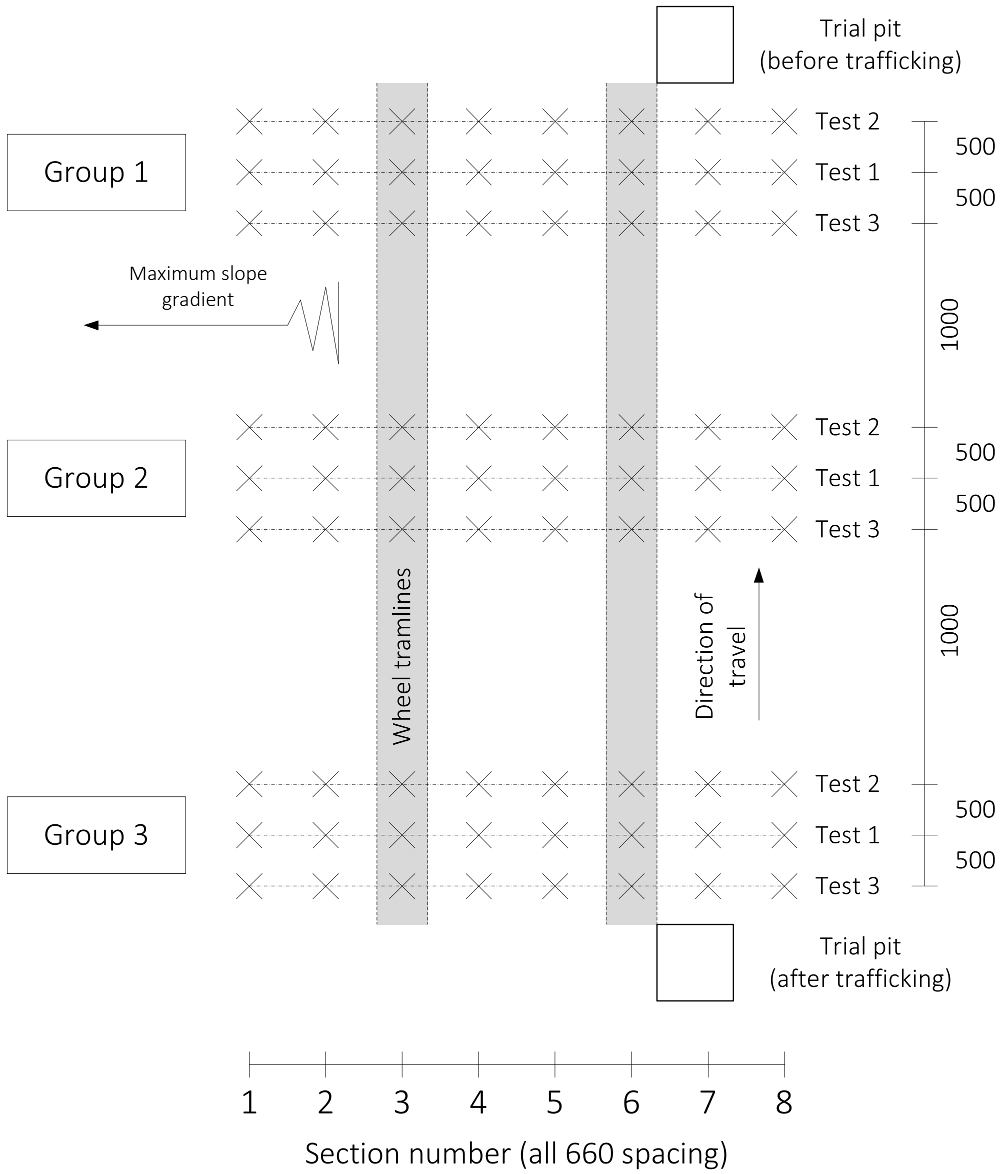

Figure 3: Experimental layout used at Sites A and B. Cross symbols show locations of individual penetrometer tests. Dimensions in mm, not to scale

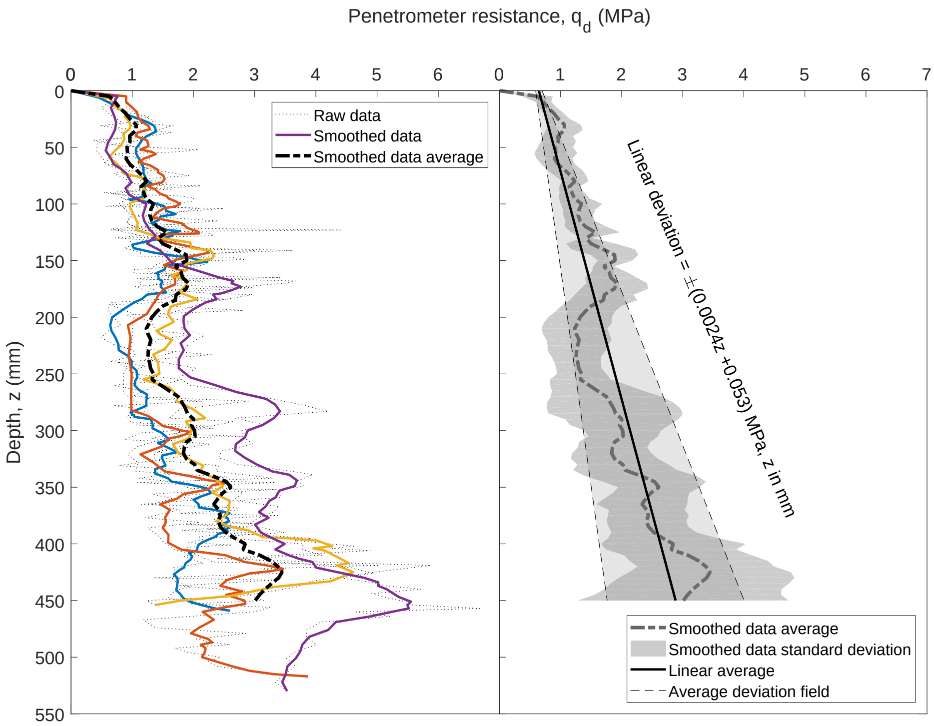

Figure 4: Laboratory penetrometer data: left) Raw and smoothed penetration profiles and average penetration resistance; right) smoothed data average penetration resistance and standard deviation and linearised average and deviation

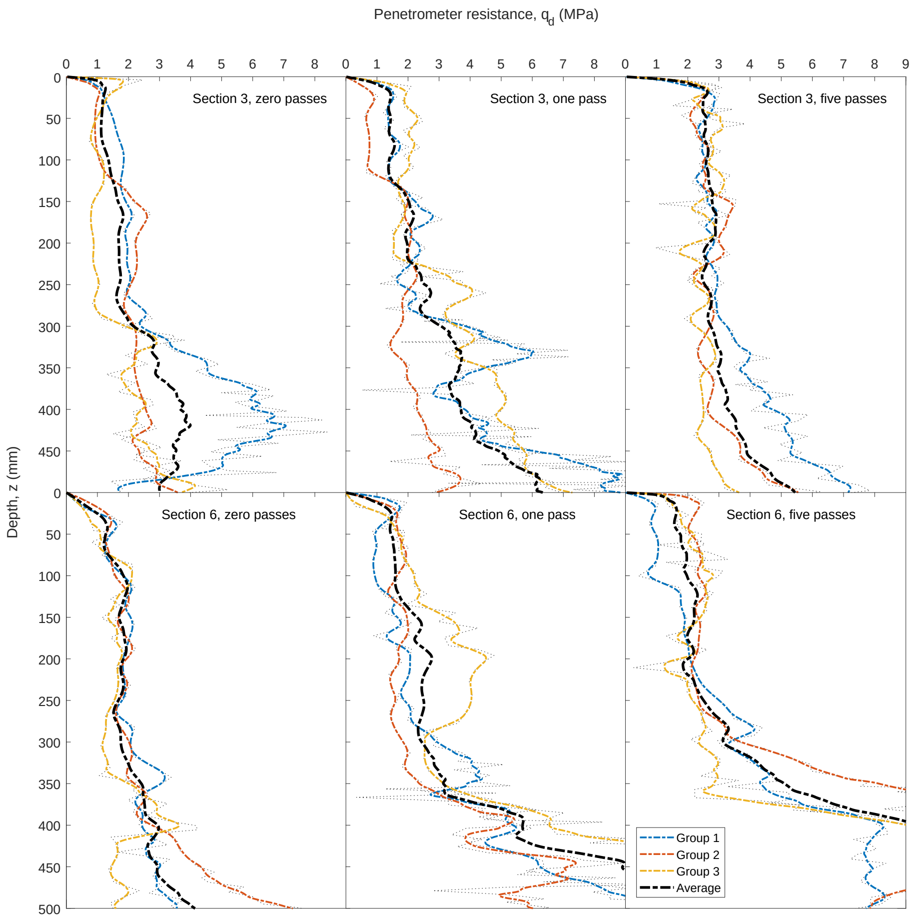

Figure 5: Site A raw, smoothed and mean penetrograms, sections 3 and 6, tests 1 to 3

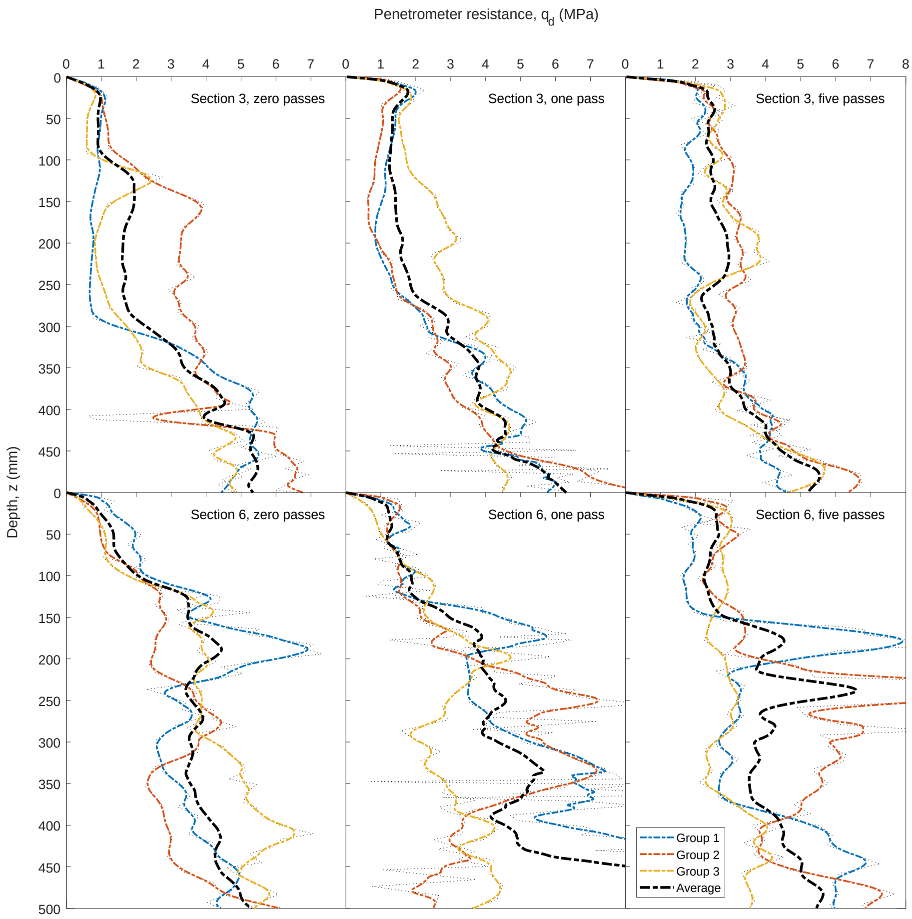

Figure 6: Site B raw, smoothed and mean penetrograms, sections 3 and 6, tests 1 to 3

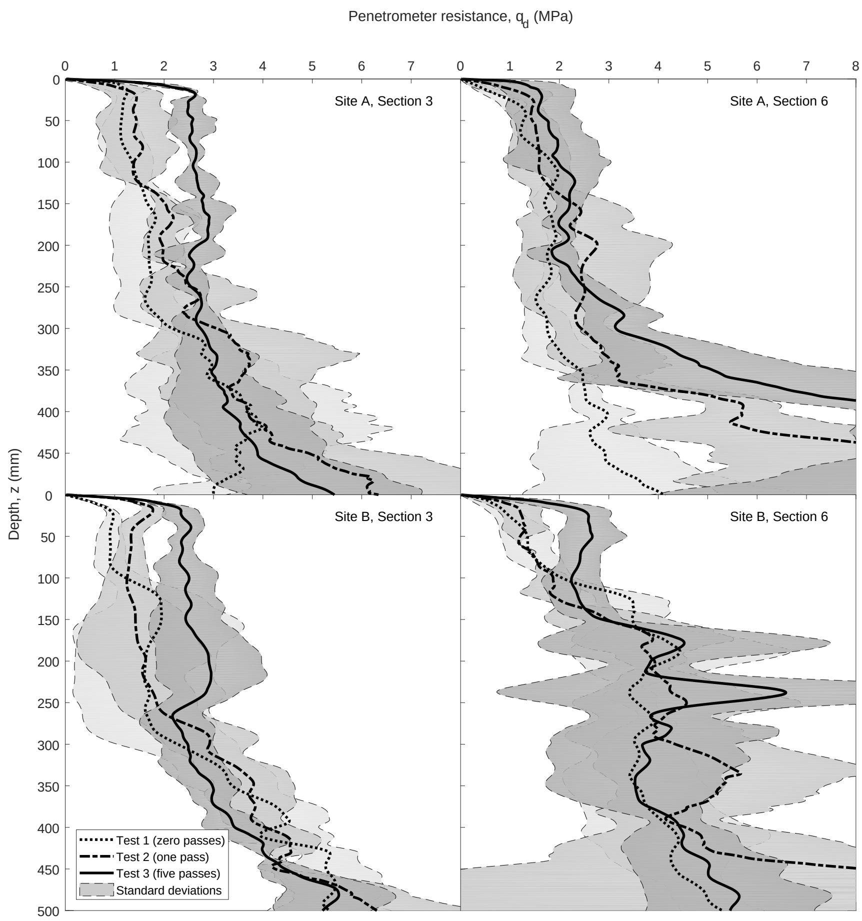

Figure 7: Site A (top) and B (bottom) average penetration resistance and standard deviation for tests 1 to 3

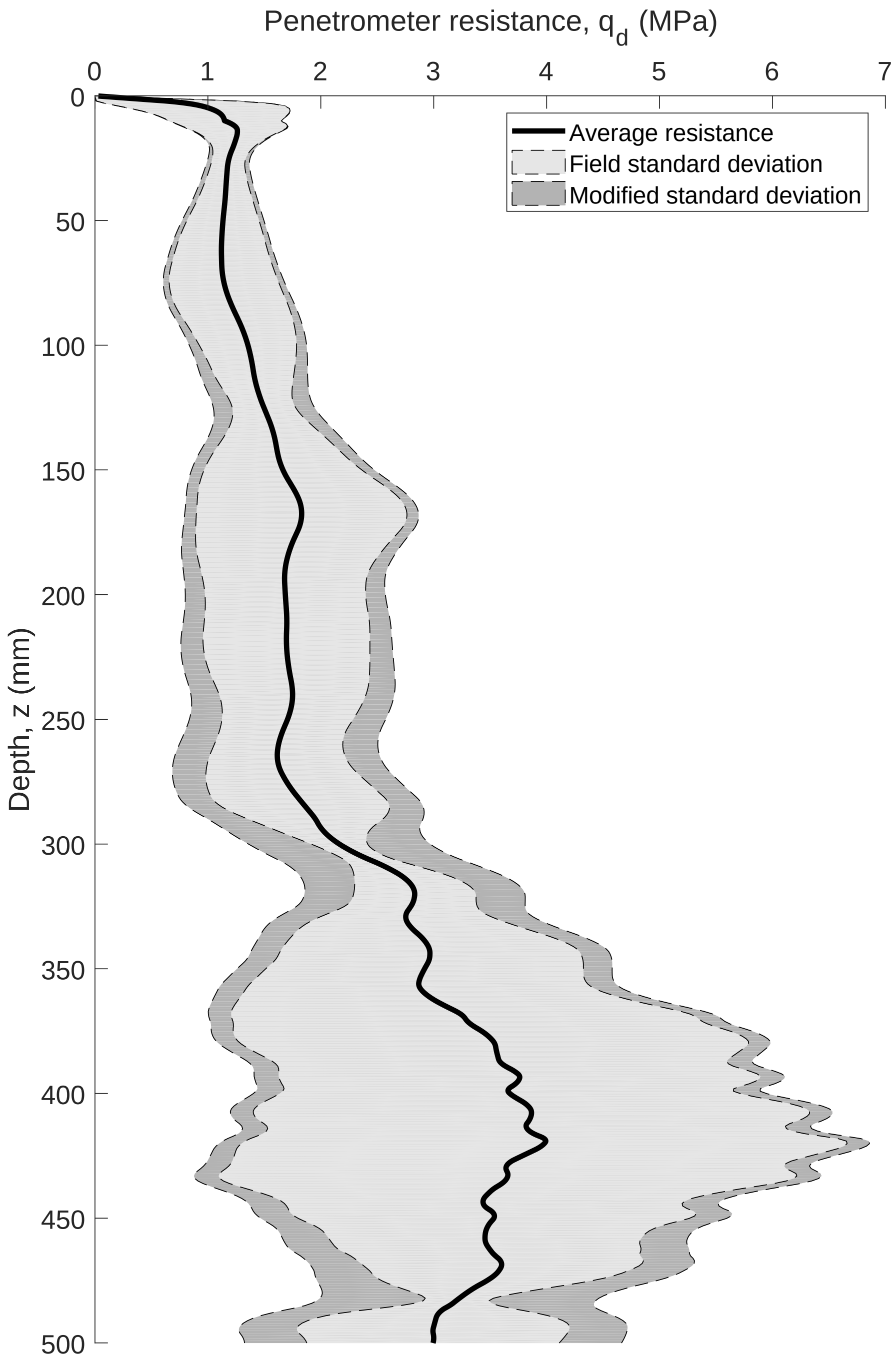

Figure 8: Example effect of device uncertainty on smoothed field data: Site A, Section 3 Test 1 (zero passes)

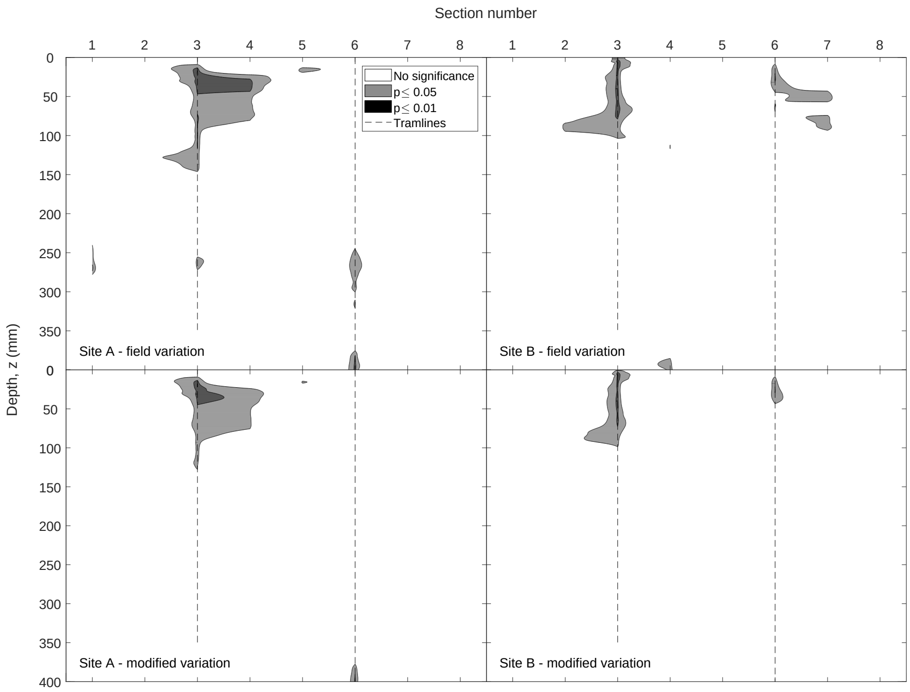

Figure 9: Paired t-test significance results for changes in measured penetration resistance between Tests 1 (zero passes) and 3 (five passes). “Field variation” denotes results obtained from measured data, “modified variation” those after including device deviation. Dashed lines show the sections immediately underneath the vehicle tyres (numbers 3 and 6)

7. Tables

Table 1: Vehicle characteristics. *Assuming level ground

Vehicle	Massey Ferguson MF6245	
Chassis	4WD	
Total mass	4230kg (with front loader)	
Track width	2 m	
	Front wheels (per wheel)	Rear wheels (per wheel)
Tyres	13.6 R24	16.9 R34
Tyre surface contact area	0.1179 m^2	0.1895 m^2
Mass distribution	828.4 kg	1331.6 kg
Surface contact pressure*	68.95 kPa (10 psi)	68.95 kPa (10 psi)

Table 2: Site A and Site B trial pit results: dry density (ρ_d); void ratio (e); water content (w); degree of saturation (S_r); and change in dry density between Tests 1 and 3 ($\Delta\rho_d$)

Site	Test	Depth (mm)	ρ_d (kgm^{-3})	e	w (%)	S_r	$\Delta\rho_d$ (%)
A	1	200	1642	0.61	5.89	0.25	-
	1	400	1651	0.60	7.14	0.31	-
	1	600	1652	0.60	7.52	0.33	-
	3	200	1781	0.49	5.15	0.28	8.46
	3	400	1817	0.46	6.45	0.37	10.06
	3	600	1778	0.49	6.51	0.35	7.59
B	1	200	1696	0.56	8.55	0.40	-
	1	400	1760	0.51	8.27	0.43	-
	1	600	1933	0.37	8.31	0.59	-
	3	200	1788	0.48	7.57	0.42	5.43
	3	400	*1717*	0.54	8.45	0.41	*-2.40*
	3	600	2095	0.26	8.57	0.86	8.36